Electro-optic measurement of the electric-field distributions in coplanar-electrode poled polymers

J. W. Wu
Department of Physics, Ewha Womans University, Seoul 120-750, South Korea

T. Wada and H. Sasabe
Frontier Research Program, The Institute of Physical and Chemical Research (RIKEN), Wako, Saitama 351-01, Japan

(Received 9 March 1994)

Electric-field distributions in coplanar-electrode configurations are studied experimentally through the linear electro-optic (EO) measurements in poled EO polymers. Thermoplastic poling of an isotropic guest-host polyimide system was employed to investigate the electrostatic factors determining the field distribution inside the EO polymer. Electrostatic analysis of the field distribution shows that the introduction of a new boundary condition formed by the polymer surface is necessary to account for field distributions measured by the linear EO effect.

PACS number(s): 42.65.Vh, 41.20.Cv, 42.70.Nq, 78.20.Jq

Polymeric materials received wide attention as electro-optic (EO) materials for their high processability and compatibility with current microelectronic techniques as well as for the intrinsic high-bandwidth response of organic molecules [1,2]. EO effect, one of the second-order nonlinear optical processes, can exist in materials lacking the centrosymmetry. In EO polymers, the centrosymmetry of polymer thin films is removed by a dc electric-field poling to achieve a macroscopic polar alignment of nonlinear optical chromophores. In thin-film samples, two configurations of electrodes are commonly adopted for the electric-field poling, parallel and coplanar (see Fig. 1). In the parallel-plate configuration, EO polymer is sandwiched between two thin electrode plates on top of a substrate (glass or silicon). In the coplanar-electrode structure, on the other hand, two thin separate electrodes with a narrow gap in between them are deposited on top of the substrate, and then EO polymer film is spin coated. Two electrode configurations seem to be equivalent as far as the dc electric poling and EO measurements are concerned. However, detailed distributions of the electric field inside polymer thin films are quite different. For a parallel-electrode configuration, the electric-field distribution is almost uniform inside the polymer film between the top and bottom electrodes, because the size of electrodes is larger than the polymer thin-film thickness. In coplanar-electrode configurations, the film covers both electrodes and the dc poling and EO effect measuring fields pass through and above the film, making the electric-field distribution complicated. Thermodynamic alignment of nonlinear optical chromophores between two electrodes follows electric-field lines which are not uniform across the gap. Even with this complication, it is important to know the electric-field distribution in coplanar electrodes. When a practical EO device is designed for light modulations, coplanar-electrode design has merit as far as processability is concerned, compared to parallel-plate electrode design. It removes at least one or two steps of the metallization process for poling and modulation operation. In addition to the practical reason, it is an interesting physics problem related to the electrostatic boundary-value problem. Since the dielectric constant of polymer films is larger than that of the air, the electric-field lines have different shapes for different thicknesses of thin films. Furthermore, the coplanar-electrode configuration with EO polymers is found to be useful for the electro-optic sampling of high-speed signal transmissions in integrated circuits [3] and also for the high-frequency light modulator [4]. In this paper, the electric-field distribution in the coplanar-electrode configuration is examined experimentally by preparing (electric-field poling) thin-film samples and measuring EO effect. Theoretical analysis of electrostatics with appropriate boundary conditions is compared with the experimental measurement and we find that there is a good agreement.

In electrostatics, the electric-field distribution is obtained from the electrostatic potential. The electrostatic potential satisfies the Laplace equation in the absence of free charges. In this case, the field distribution is determined solely from the boundary conditions. For two electrodes with a finite potential difference, the electric-field distribution is given in an elementary way. It is im-

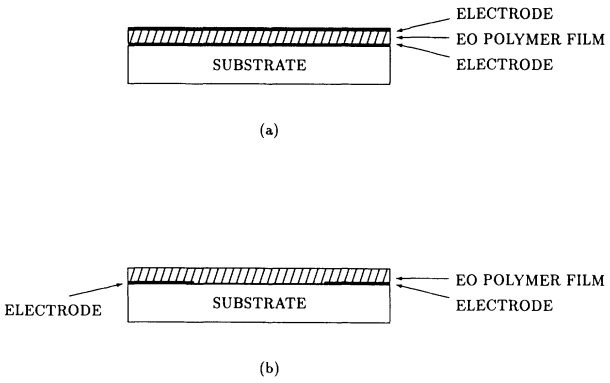

FIG. 1. Two electrode configurations commonly adopted for EO polymer films. EO polymer is sandwiched between the top and the bottom electrodes in the parallel-plate electrode configuration (a), while EO polymer is positioned on top of coplanar electrodes with a narrow gap on substrate in the coplanar-electrode configuration (b).

portant, however, to note that the presence of the polymer film itself distorts the field lines due to the introduction of a new boundary condition. Dielectric constants of polymer films being different from that of the air, the presence of a film on top of a conductor (electrodes) provides another boundary condition for the Laplace equation. One way to solve the boundary-value problem like this is to introduce image charges. The image-charge method is very useful for the geometrically symmetric electrodes, which is the case for coplanar electrodes. The position and size of the image charges depend on the thickness and the dielectric constant of the polymer film [5]. Figure 2 shows the computer plotting of the simulated electric-field distribution for a thick polymer film when the proper image charge and the dielectric constant of the polymer film are taken into account. Field strength gradually decreases as the vertical distance from the substrate increases. Field components along the substrate, responsible for the EO effect in the coplanar-electrode configuration, also are not uniform across the gap. These variations will lead to a change of EO effects for films with different thicknesses.

To study the electric-field distribution experimentally from EO measurement, we employed a guest-host polyimide system. Since we are interested in the field distribution, we should be careful in selecting a model system to get rid of effects other than electrostatics. Structural anisotropy inherent to polymer films and charge concentration near electrodes, for example, may distort the electric-field distribution. To minimize the structural anisotropy we chose the LQ2200 compound (Hitachi Chemical Co.) as the host polyimide system, which is known to possess an isotropic structure (optically and dielectrically) [6]. Furthermore, the guest-host polyimide system should have a sufficient thermal stability of EO response at room temperatures after poling to study the field distribution [7]. In this regard, a stilbene dye, 4-(dicyanomethylene)-2-methyl-6-(*p*-dimetylaminostyryl-4*H*-pyran) (DCM) molecule was chosen as guest nonlinear optical molecules [9]. The DCM-LQ2200 guest-host system is known to possess a good thermal stability of EO response in both through-imidization (thermosetting) and postimidization (thermoplastic) poling [7,8]. Compared with the through-imidization poling, the electric current monitoring during poling shows that the postimidization (thermoplastic) poling near the glass transition temperature minimizes the ion transport occurring during electric-field poling. Through-densification (thermosetting) poling [10], the other poling process possible in polyimide systems, cannot be employed in the DCM-LQ2200 system due to the limited thermal stability of chemical bonds in DCM chromophores at the densification temperatures exceeding 300 °C. Based on these considerations we chose an 8% solid solution DCM-LQ2200 guest-host polyimide as the material system and we adopted the post-imidization (thermoplastic) poling for the electric-field poling. It is known that charge injection occurs in the coplanar-electrode configuration when the dc poling field is applied at temperatures above the glass transition temperature T_g of polymer [11]. Sometimes the charge injection seems to lead to an apparent enhancement of EO response [12]. In order to take care of this charge injection problem, we kept the poling temperature at least 50 °C below T_g. According to Valley *et al.* [7], T_∞ appearing in the Williams-Landle-Ferry equation is in the range of 197 °C and 207 °C for the 5% and 10% guest contents in LQ2200 hosts. T_∞ is usually about 50 °C below T_g [13], hence T_g will be about 250 °C for an 8% solid solution DCM-LQ2200 system. In fact, T_g, not T_∞, is the temperature where the α relaxation of the polymer backbone occurs related to the glass-rubber transition [14].

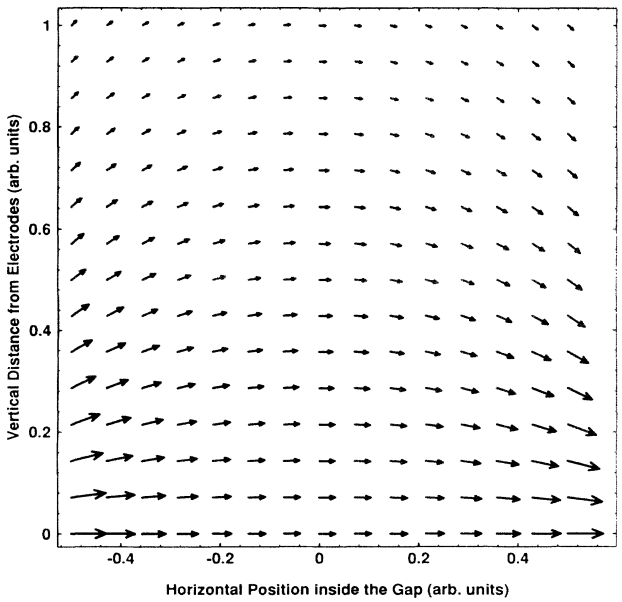

FIG. 2. Computer-simulated plot of electric-field lines in coplanar-electrode configuration. x axis (abscissa) and y axis (ordinate) are equally scaled. Coplanar electrodes (not shown here) are placed on the left ($x=-1.0$) and right ($x=+1.0$) bottom. The dielectric constant ϵ of polymer thin film is taken as 3.4 [6]. The position of image charge is on the mirror-reflected point of the electrodes with respect to the polymer thin-film top surface, plane of $y=+1.0$. That is, in this particular example the film thickness is half of the electrode gap size. The magnitude of the image charge is $(\epsilon-1)/(\epsilon+1)$.

In preparing samples, 10-μm-gap coplanar chromium electrodes were patterned on top of fused quartz. The thickness of electrodes was around 5000 Å, which is much smaller than the gap size of the coplanar electrodes. An 8% weight concentration of DCM in LQ2200 polyimide was prepared by overnight stirring of DCM in LQ2200 polyamic acids. In order to study the electric-field distribution vertical to the electrode plane, six samples were prepared. Sample 1 has the EO polymer (DCM-LQ2200) of 2 μm thickness right on top of the coplanar electrodes. After curing at 250 °C for half an hour, it was poled at the poling field strength of 50 V/μm at 200 °C (about 50 °C below T_g) for 1 min to minimize the charge injection. In sample 2, the base polymer with thickness of 2 μm was spin coated on top of coplanar electrodes and fully cured at 300 °C. After that, the same EO polymer was spin coated on top of the fully cured

bare polymer, and cured again at 250 °C for half an hour. The poling was performed at the identical condition as sample 1. The same step was repeated for samples 3–6; only the bare polymer thickness increased through successive spin coating and curing. In this way, EO polymer of the same thickness is positioned on top of the electrodes with different vertical distance from the electrode, bare polymer films providing different spacings. Film stack configuration of sample 6, for example, is shown in Fig. 3. EO effect comes from the active EO polymer on the top layer, while the base polymer just sits there to provide vertical spacing between the electrode and the EO polymer, enabling us to study the electric-field distribution.

Since the EO signal has a good thermal stability at room temperature, it is easy to do the EO measurement and compare the signals. The cross-polarizer lock-in technique was employed to measure the EO response [8,15]. Figure 4 shows the measured EO signal as a function of the film thickness. Nonlinear optical molecules residing inside the EO polymer give rise to the measured EO signal, the magnitude providing information on the field distributions in the top layer. That is, the electric-field distribution determines both the orientational distribution function of guest molecules and the amount of detected EO response. Different thickness samples will sample the field distribution at different vertical positions above the coplanar electrodes. As expected, the EO signal decreases rapidly as the film gets thicker.

From the simple variation of the field distribution, two effects accumulate to result in a large difference in the EO effect for films with different thicknesses. First, most importantly, the orientational distribution of nonlinear optical molecules is different. The ratio of the dipolar interaction energy to the thermal energy, $x=\mu E_p/kT$, varies inside the polymer film since the electric-field distribution is not uniform. This means that one single distribution function cannot describe the thermodynamic molecular alignment properly. In other words, the order parameter related to the achieved alignment of the nonlinear optical molecules varies as a function of the vertical distance from the substrate as well as the lateral position inside the gap. The second effect, equally important, comes in when the linear EO effect is measured. Change of the refractive index experienced by an optical light on the application of a dc field E_k^0, which is the very EO effect, is described by an effective linear polarizability α_{ij}^{eff}.

$$\alpha_{ij}^{\text{eff}}(-\omega;\omega;0)=\chi_{ijk}^{(2)}(-\omega;\omega,0)E_k^0 .$$

For a given field distribution of the modulating electric field E_k^0, the amount of refractive index change is not homogeneous across the gap between two electrodes. Distortion of the electric-field results in the distortion of the index changes accordingly. These two effects combine to give an overall variation on the EO effect for coplanar-electrode poled polymer thin films with different thicknesses. Since both the preparation (poling) of samples and the measurement of EO effect involve dc electric fields, the distortion effect is doubled, giving an enhanced effect in the end. The phase-shift difference $\Delta\phi=\phi_{\parallel}-\phi_{\perp}$ between the parallel and perpendicular components of a linearly polarized light along 45° relative to the poling field direction can be expressed in terms of the EO molecular hyperpolarizability $\beta_{ijk}(-\omega;\omega,0)$. For a linearly shaped molecule like DCM, $\beta_{333}(-\omega;\omega,0)$, the principal axis component along the molecular axis, is dominant. In the lowest order, $\Delta\phi$ is [16,17]

$$\Delta\phi \propto \beta_{333}(-\omega;\omega,0)\frac{\mu E_p}{kT}E^0 .$$

Here both the poling field E_p and the measuring field E^0 have distorted field distribution as shown in Fig. 2, while the optical field E^{ω} passing through the film is not affected by field distortions. In estimating the distorted electric-field distribution from electrostatics the spatial variation across the 10-μm gap is averaged since the focused beam spot size was not small enough as well as our interest lies only on the vertical variation of EO signal for different thickness thin films. Algebraic sum of squared values of horizontal components of electric fields shown in Fig. 2 provides the theoretical EO signal for one EO polymer film. In Fig. 5, these calculated magnitudes of EO signal (closed circles) are drawn for EO polymer thin films with different thickness base polymer. Also drawn are the algebraic sum of electric-field horizontal components (open circles), not the squared values, for comparison. It is obvious that the measured EO signals are in good agreement with the calculated EO signals. This suggests that distortion of the electric fields in coplanar electrodes affects both the orientational distributions of chromophores and the EO measurements, resulting in quite reduced overall signals for thick films.

Second-harmonic generation (SHG) experiment will

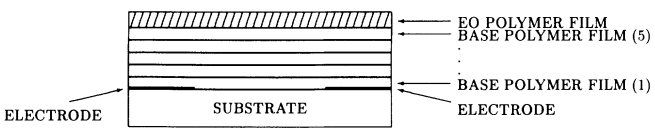

FIG. 3. Film stack configuration of sample 6 is shown. On top of the coplanar electrodes, five base polymer films (1)–(5) are spin coated and fully cured successively. Thereafter, EO polymer (top layer) is spin coated, cured, and poled.

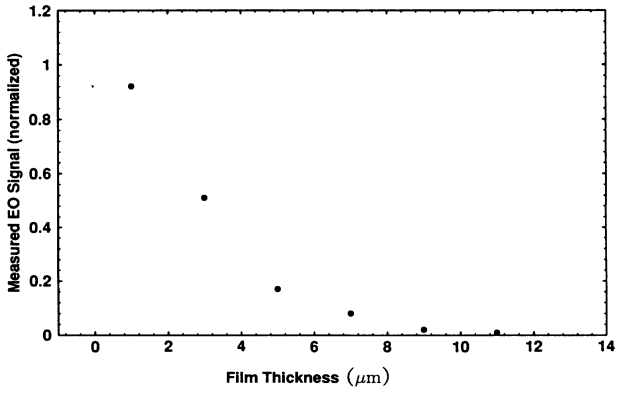

FIG. 4. Measured EO signal using a cross-polarizer lock-in technique for different thickness polymer films.

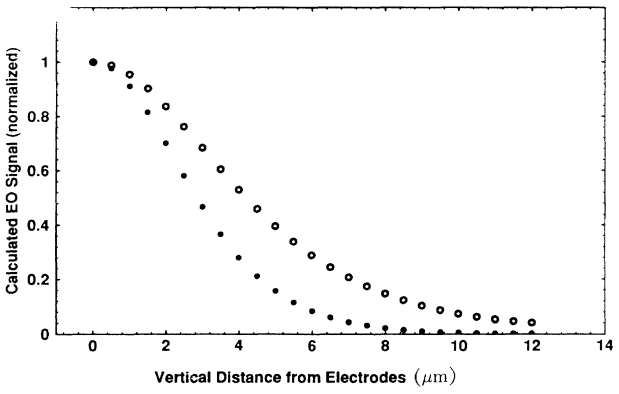

FIG. 5. Calculated EO signal (closed circles) for different thickness polymer films. The magnitude decreases rapidly as the film thickness increases. Calculated electrostatic fields along the substrate plane (open circles) are shown for comparison.

separate out the poling effect and the EO coefficient measurement effect. Fundamental light goes through the film without being affected by the electric-field distribution of the electrode configuration for poling. Macroscopic SHG polarization is

$$p_3^{2\omega} \propto \beta_{333}(-2\omega;\omega,\omega)\frac{\mu E_p}{kT}E_3^{\omega}E_3^{\omega} ,$$

where only the poling field E_p not the measuring fundamental optical field E_3^{ω}, is distorted by the coplanar electrodes. Therefore SHG signals will decrease much more slowly as the film thickness increases for the same coplanar-electrode poled sample. In other words, SHG signals will be the open circles of Fig. 5.

In summary, electric-field distributions in coplanar-electrode configurations are investigated by measuring electro-optic response in a poled DCM-LQ2200 guest-host polyimide system. Electro-optic effects for films with different thicknesses provide information on the field distributions. Rapid decrease of the measured electro-optic response as the film thickness increases agrees well with the calculated electric-field distributions when proper boundary conditions are taken into account.

We gratefully thank T. Imai for providing the fused quartz cells with coplanar-electrode patterns. J.W.W. would like to thank RIKEN for the hospitality during the visit to RIKEN. The work of J.W.W. was supported by Korea Science and Engineering Foundations (Grant No. 931-0200-010-2) and Basic Science Research Institute Program, Ministry of Education, Republic of Korea (Grant No. BSRI-94-2428).

[1] See, for example, *Nonlinear Optical Properties of Organic Materials IV,* edited by K. D. Singer, SPIE Conf. Proc. Vol. No. 1560 (The International Society for Optical Engineering, Bellingham, WA, 1991).

[2] A. F. Garito, J. W. Wu, G. F. Lipscomb, and R. Lytel, in *Advanced Organic Solid State Materials,* edited by L. Y. Chiang, P. Chaikin, and D. O. Cowan, MRS Symposia Proceedings No. 173 (Materials Research Society, Pittsburgh, 1990), p. 467.

[3] J. I. Thackara, D. M. Bloom, and B. A. Auld, Appl. Phys. Lett. **59**, 1159 (1991).

[4] O. Solgaard, F. Ho, J. I. Thackara, and D. M. Bloom, Appl. Phys. Lett. **61**, 2500 (1992).

[5] J. D. Jackson, *Classical Electrodynamics,* 2nd ed. (Wiley, New York, 1975).

[6] Hitachi Chemical Data Sheet, Hitachi Chemical Co., Ltd. (1983).

[7] J. F. Valley, J. W. Wu, S. Ermer, M. Stiller, E. S. Binkley, J. T. Kenney, G. F. Lipscomb, and R. Lytel, Appl. Phys. Lett. **60**, 160 (1992).

[8] J. W. Wu, J. F. Valley, S. Ermer, E. S. Binkley, J. T. Kenney, G. F. Lipscomb, and R. Lytel, Appl. Phys. Lett. **58**, 225 (1991).

[9] S. Ermer, J. F. Valley, R. Lytel, G. F. Lipscomb, T. E Van Eck, and R. Lytel, Appl. Phys. Lett. **61**, 2272 (1992).

[10] J. W. Wu, E. S. Binkley, J. T. Kenney, R. Lytel, and A. F. Garito, J. Appl. Phys. **69**, 7366 (1991).

[11] M. Stahelin, D. M. Burland, M. Ebert, R. D. Miller, B. A. Smith, R. J. Twieg, M. Volksen, and C. A. Walsh, Appl. Phys. Lett. **61**, 1626 (1992).

[12] S. Yitzchaik, G. Berkovic, and V. Krongauz, J. Appl. Phys. **70**, 3949 (1991).

[13] J. D. Ferry, *Viscoelastic Properties of Polymers,* 3rd ed. (Wiley, New York, 1980).

[14] N. G. McCrum, B. E. Read, and G. Williams, *Anelastic and Dielectric Effects in Polymeric Solids* (Wiley, New York, 1967).

[15] C. C. Teng and H. T. Man, Appl. Phys. Lett. **56**, 1734 (1990).

[16] K. D. Singer, M. G. Kuzyk, and J. E. Sohn, J. Opt. Soc. Am. B **4**, 968 (1987).

[17] J. W. Wu, J. Opt. Soc. Am. B **8**, 142 (1991).